© 2014. Published by The Company of Biologists Ltd | The Journal of Experimental Biology (2014) 217, 3365-3376 doi:10.1242/jeb.105338

RESEARCH ARTICLE

The search space of the rat during whisking behavior

Lucie A. Huet[1] and Mitra J. Z. Hartmann[1,2,*]

ABSTRACT

Rodents move their vibrissae rhythmically to tactually explore their surroundings. We used a three-dimensional model of the vibrissal array to quantify the rat's 'search space' during whisking. Search space was quantified either as the volume encompassed by the array or as the surface formed by the vibrissal tips. At rest, the average position of the vibrissal tips lies near the rat's mouth, and the tips are all approximately equidistant from the midpoint between the rat's eyes, suggesting spatial registration with the visual system. The intrinsic curvature of the vibrissae greatly increases the volume encompassed by the array, and during a protraction, roll and elevation changes have strong effects on the trajectories of the vibrissal tips. The size of the rat's search space – as measured either by the volume of the array or by the surface area formed by the vibrissal tips – was surprisingly unaffected by protraction angle. In contrast, search space was strongly correlated with the 'spread' of the array, defined as the angle between rostral and caudal-most whiskers. We draw two conclusions: first, that with some caveats, spread can be used as a proxy for changes in search space, and second, in order to change its sensing resolution, the rat must differentially control rostral and caudal vibrissae. Finally, we show that behavioral data can be incorporated into the three-dimensional model to visualize changes in vibrissal search space and sensing resolution during natural exploratory whisking.

KEY WORDS: Whisker, Vibrissa, Trigeminal, Superior colliculus, Active touch, Sensing volume

INTRODUCTION

During tactile exploratory behavior, rats sweep their vibrissae (whiskers) back and forth in a rapid, rhythmic motion called 'whisking' (Vincent, 1913; Welker, 1964; Berg and Kleinfeld, 2003). Whisking movements are often synchronized and symmetric between the two sides of the face, and they have an extraordinarily precise frequency (8 Hz) when averaged over many cycles (Carvell and Simons, 1990; Fee et al., 1997; Gao et al., 2001; Harvey et al., 2001; Berg and Kleinfeld, 2003; Sachdev et al., 2003). Studies that have exploited these spatiotemporal regularities have shed considerable light on sensorimotor integration during vibrissal active touch.

At the same time, other studies have highlighted the complex kinematics of whisking and its rich variability during exploratory behavior (Wineski, 1983; Wineski, 1985; Carvell and Simons, 1990; Carvell and Simons, 1995; Bermejo et al., 2002; Sachdev et al., 2003; Sellien et al., 2005; Towal and Hartmann, 2006; Mitchinson et al., 2007; Knutsen et al., 2008; Towal and Hartmann, 2008; Grant et al., 2009; Deutsch et al., 2012; Grant et al., 2012; Mitchinson and Prescott, 2013). The dominant rostral–caudal whisking motion is coupled to changes in dorso-ventral elevation (Bermejo et al., 2002) as well as to roll of the whisker about its own axis (Knutsen et al., 2008). Rats can vary whisking amplitude and velocity, and contact with an object strongly affects subsequent whisking motions. Whiskers on the right and left sides can move asymmetrically and asynchronously, and rostral and caudal whiskers on a single side of the face can sometimes move independently.

Whisking is thus a fundamentally rhythmic behavior but sufficiently flexible to accommodate a variety of task requirements. Behavioral studies have suggested that a large fraction of the variance in whisking patterns can be explained by two principal components: (1) the average protraction angle, and (2) the 'spread' of the whiskers, defined as the angular difference between the rostral-most and caudal-most whiskers, as measured in a top-down camera view (Grant et al., 2009).

Although these two parameters (protraction angle and spread) are relatively easy to observe during behavioral experiments, they are essentially one-dimensional measures of whisking motion. They do not quantify the complex, three-dimensional (3D) regions of space that the rat can search with its vibrissae or the two-dimensional (2D) surfaces formed as the tips of the whiskers contact an object.

The size of the vibrissal 'search space' can be quantified either as the total volume encompassed by the array (in cm^3) or as the surface area formed by the vibrissal tips (in cm^2). Because the vibrisssae have intrinisic curvature and exhibit complex kinematics, one might *a priori* expect the search space to exhibit a strong non-linear dependence on protraction angle, the spacing of vibrissae within the array, and spread.

In the present study, we first used a 3D model of the rat head and vibrissal array to investigate the answers to three closely related questions: (1) what is the shape of the vibrissal search space, and how does it change over a protraction?; (2) how is the search space affected by intrinsic curvature, roll, and elevation?; and (3) how do protraction angle, spacing and spread affect the size of the search space? We then inserted behavioral data into the 3D anatomical model to visualize the search space during natural whisking. Combining behavioral data with simulations allowed us to observe the effects of variable amplitude whisking, right–left asymmetries, and rostral–caudal amplitude and phase differences.

RESULTS

The 3D morphology of the rat head and vibrissal array at rest was based on Towal et al. (Towal et al., 2011) and Knutsen et al. (Knutsen et al., 2008). The morphology included the positions of the vibrissal base points and the shapes and orientations of the vibrissae.

As described in Materials and methods, the two datasets (Towal et al., 2011; Knutsen et al., 2008) provide slightly different resting angles for elevation (φ). The primary reason is that Towal et al. obtained measurements of all resting angles using euthanized rats, while Knutsen et al. measured the elevation angles at the start of a whisk in awake behaving rats. All analyses involving the vibrissal array at rest were therefore performed twice, using the two different elevation

[1]Department of Mechanical Engineering, Northwestern University, Evanston, IL 60208, USA. [2]Department of Biomedical Engineering, Northwestern University, Evanston, IL 60208, USA.

*Author for correspondence (hartmann@northwestern.edu)

Received 12 March 2014; Accepted 9 June 2014

The Journal of Experimental Biology (2014) doi:10.1242/jeb.105338

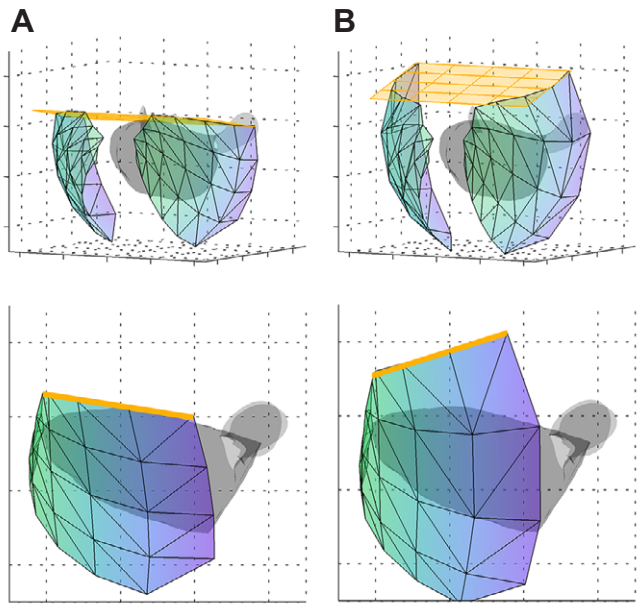

Fig. 1. The tips of the A-row vibrissae form a plane above the rat's head. In each subplot, the surfaces formed by all rows of vibrissa are shown as a triangular mesh in blue and green, and the planar fits to the tips of the A-row vibrissae are in orange. The gray body in the background represents the rat's head. (A) The planar fit using the elevation angles established in Towal et al. (Towal et al., 2011). The fit has an average error of 0.4 mm. (B) The planar fit using the elevation angles from Knutsen et al. (Knutsen et al., 2008). This fit yields an average error of 0.64 mm. All subplots use the perceptually balanced color map from Niccoli (Niccoli, 2010), and the side of a grid square represents 20 mm.

values. Simulations involving whisking motions used roll and elevation values from Eqn 2A–E (see Materials and methods), while the value of protraction angle θ was varied to simulate a whisk.

When the array is at rest, the tips of the dorsal vibrissa form a plane that 'clears' the rat's head

We began by evaluating the shape of the vibrissal array when the whiskers are at rest. As shown in Fig. 1, the tips of the A-row vibrissae approximate a plane, regardless of whether the parameters for elevation are obtained from Towal et al. (Towal et al., 2011) or from Knutsen et al. (Knutsen et al., 2008). Using either set of parameters, the plane clears the top of the rat's head.

Fig. 1A shows that if elevation parameters from Towal et al. (Towal et al., 2011) are used, the tips of the A-row vibrissae only just barely clear the head. The plane they form is approximately tangent to the rat's head above the eyes. In contrast, when the elevation parameters from Knutsen et al. (Knutsen et al., 2008) are used, the tips of the A-row vibrissae extend well above the top of the head and even above the ears, and the plane they form slopes downwards, towards the nose of the rat.

Notably, the A-row elevation values are the most different between the two data sets (see Table 1). Thus, the two planar fits shown in Fig. 1 illustrate the result of the present study that differs the maximum amount between the two models.

Regardless of which parameter set is used, the E-row vibrissae (Table 1) extend well below the rat's head. It is therefore evident that the vibrissae tips completely surround the rat's head, even when the vibrissae are at rest. The vibrissae cover the space not only to the sides of the rat's head, as would be expected, but also above and below. The dorsal–ventral asymmetry of the volume enclosed by the vibrissae tips is likely explained by the position of the rat's eyes, as described next.

The surface formed by the tips of the vibrissae at rest resembles a section of a sphere centered on the rat's eyes

Fig. 2 illustrates geometric fits to the tips of all the vibrissae. Fig. 2A,B illustrates spherical and ellipsoid fits to the tips of the vibrissae at rest, as established by the values in Towal et al. (Towal et al., 2011), and Fig. 2C,D shows fits using the resting elevation values from Knutsen et al. (Knutsen et al., 2008). Parameters for the fits are provided in Table 2. None of the fits were found to be significantly different from each other ($P>0.1$, two-tailed t-test). The radii from the fits using elevation values from Knutsen et al. tend to be slightly larger than the radii obtained using data from Towal et al. Compared with the spherical fits, both ellipsoid fits are slightly elongated in the dorsal–ventral direction and reduced in the rostral–caudal direction. The top of the ellipsoid using the Towal et al. elevation parameters is tilted rostrally by 1.5 deg, and the top of the ellipsoid using the Knutsen et al. elevation parameters is tilted caudally by 0.3 deg.

Fig. 2 also illustrates that the centroid (i.e. the average position) of the vibrissae tips lies near the mouth. Intriguingly, however, all the fits in Fig. 2 are centered approximately at the midpoint between the rat's eyes. In other words, the average position of the vibrissae tips is at the rat's mouth, but the vibrissae tips are all nearly equidistant from the midpoint between the rat's eyes.

During a protraction, the surface defined by the whisker tips becomes flatter but never quite forms a plane

We next aimed to obtain an estimate of the shape of the surface formed by the whisker tips over the course of a protraction. The results are shown in Fig. 3A. To run these simulations, we used the simulation tool PuppetMaster, described in Materials and methods and provided as a MATLAB code (available on request from the corresponding author). Both sides of the array were included in the fit, resting elevation values were those from Knutsen et al. (Knutsen et al., 2008), and all simulations included both roll and elevation of the whiskers as described in Eqn 2 in Materials and methods.

The third and fourth subplots of Fig. 3A reveal that the two-sided fit breaks down near a protraction angle θ≈40 deg. After θ≈53 deg the ellipsoid fit no longer recognizably represents the vibrissae tips (mean error >4.0 mm).

Table 1. Resting elevation angles (average per row)

Row	φ_{rest} from Towal et al., 2011 (deg)	φ_{rest} from Knutsen et al., 2008 (deg)	Magnitude of the difference |Knutsen φ_{rest} – Towal φ_{rest}| (deg)
A	33.1	56	22.9
B	17.1	25	7.9
C	1.0	−4.2	5.2
D	−15.7	−27.2	11.5
E	−33.1	−44	10.9

The Journal of Experimental Biology (2014) doi:10.1242/jeb.105338

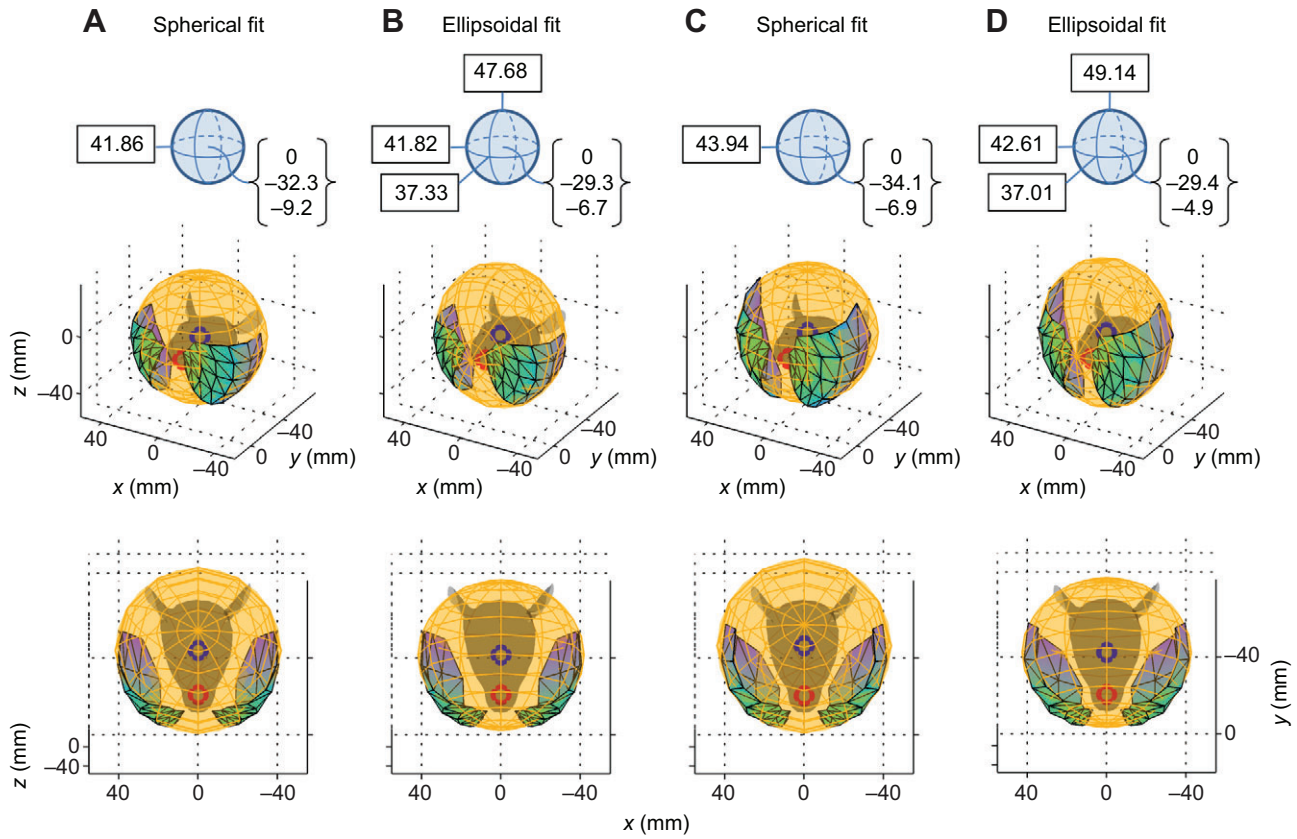

Fig. 2. Geometric fits to the tips of the vibrissae at rest. The top row depicts sphere and ellipsoid centers and radii in dimensions of mm. (A,B) Data from Towal et al. (Towal et al., 2011); (C,D) data from Knutsen et al. (Knutsen et al., 2008). For A and C, the number to the left of the spherical icon indicates the radius of the sphere. The bracketed set of numbers represents the center of the spherical fit in (*x*, *y*, *z*) coordinates. For B and D, three numbers in boxes surround the spherical icon. Counter-clockwise from the top, these numbers indicate the ellipsoid radius in the dorso-ventral, medio-lateral and rostro-caudal directions, respectively. The bracketed set of numbers to the right of each icon represents the center of the ellipsoidal fit in (*x*, *y*, *z*) coordinates. The middle and bottom rows show two views of each fit. The blue circle represents the center of the sphere or ellipsoid, and the red circle represents the centroid of the vibrissae tips.

Fig. 3A also shows that over the course of a protraction, the ellipsoid moves forward, flattens in the rostral–caudal direction, and elongates in the medio-lateral direction. These results are quantified in Fig. 3B,C. Fig. 3B plots the rostral–caudal position of the center of the ellipsoid as well as the position of the centroid of the vibrissal tips over protraction. The ellipsoid begins centered near the midpoint of the eyes and moves more rostral until θ≈35 deg, when the two-sided fit begins to break down. The centroid of the vibrissal tips shifts more rostral in a linear fashion, well past 40 deg. Fig. 3C illustrates that the tips of the vibrissae form a flatter surface over the course of a protraction. Flatness was calculated by dividing the mean of the two largest ellipsoid radii by the shortest radius. The shortest radius always pointed approximately in the rostral–caudal direction.

Because the ellipsoid fit to two sides of the array broke down before the protraction was complete, we next performed an ellipsoid fit using only a single side of the array, again with the goal of obtaining a quantitative description of the surface formed by the vibrissal tips over the entire course of a protraction. Parameters for

Table 2. Spherical and ellipsoid fits to the tips of the vibrissae at rest

	Towal et al., 2011		Knutsen et al., 2008		
	Spherical fit, both sides	Ellipsoid fit, both sides	Spherical fit, both sides	Ellipsoid fit, both sides	Ellipsoid fit, single side
R–C radius (mm)	41.9	37.3	43.9	37.0	31.9
M–L radius (mm)	N/A	41.8	N/A	42.6	18.8
D–V radius (mm)	N/A	47.7	N/A	49.1	39.0
Ellipsoid pitch (deg)	N/A	1.5	N/A	−0.3	N/A
Mean error (mm)	1.79	1.51	2.19	1.44	0.714
Median error (mm)	1.12	0.89	1.44	0.96	0.550
Center (*x*, *y*, *z*) (near the eyes) (mm)	(0, −32.2, −9.2)	(0, −29.3, −6.7)	(0, −34.1, −6.9)	(0, −29.4, −4.9)	(±20.7, −26.0, −12.1)
Centroid of tips (near the mouth) (mm)	(0, −10.8, −15.4)	(0, −10.8, −15.4)	(0, −9.97, −14.1)	(0, −9.97, −14.1)	(±22.2, −9.97, −14.1)

The last column shows parameters for an ellipsoid fit to a single side of the array only. None of the fits to both sides of the array were significantly better than any of the others, but unsurprisingly, the single-sided fit is significantly better (P<0.05) than any of the two-sided fits.
R–C, rostral–caudal; M–L, medial–lateral; D–V, dorsal–ventral.

The Journal of Experimental Biology (2014) doi:10.1242/jeb.105338

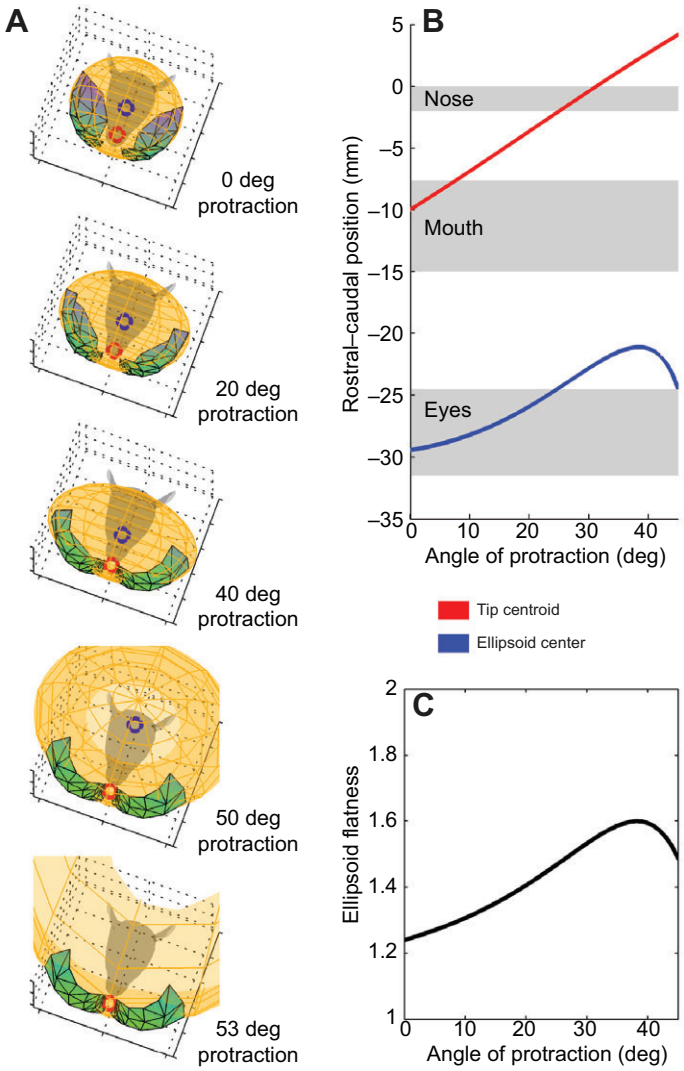

Fig. 3. The bilateral ellipsoid fit to the vibrissa tips flattens and translates rostrally during protraction until the fit breaks down near 40 deg protraction. (A) Ellipsoid fit to both sides of the array shown at five stages of protraction. (B) Rostral–caudal position of the centroid of the tips and the center of the ellipsoid. (C) Ellipsoid flatness, calculated as the ratio of the mean of the two largest radii and the smallest radius.

this fit with the vibrissae at rest are shown in the right-most column of Table 2.

Fig. 4 illustrates ellipsoid fits to the tips of the vibrissae on a single side of the array. Over the entire protraction (80 deg), the mean error was 3 mm or less at each time step, representing at most 8% of the mean of the current ellipsoid radii. As shown in the first plot of Fig. 4A, when the vibrissae are at rest, the longest radius is oriented dorso-ventrally, and the shortest radius is oriented medio-laterally. The curve shown in Fig. 4B is the azimuthal angle of the shortest radius's axis and represents the direction of the vector normal to the flattest face of the ellipsoid. As in the case of the double-sided fit, over the course of a protraction the surface formed by the tips orients to become larger medio-laterally and becomes flatter (Fig. 4C).

Fig. 4D illustrates that even at an extreme angle of protraction (θ=80 deg), however, the tips of the vibrissae do not form a plane. An ellipsoidal fit is still significantly better ($P<0.05$, two-tailed t-test). The primary reason is that the rostral vibrissae are not long enough to match the distance subtended by the more caudal whiskers when fully protracted.

Intrinsic vibrissal curvature increases the volume of the rat's search space, but roll and elevation have only a small effect on volume

In all the results presented so far, the whiskers were simulated to have an intrinsic curvature approximating a parabola in order to match the natural shape of real rat vibrissae (Knutsen et al., 2008; Towal et al., 2011; Quist and Hartmann, 2012). Additionally, all simulations of whisking have included the effects of elevation and roll from Eqn 2 in Materials and methods (Bermejo et al., 2002; Knutsen et al., 2008). We next examined how intrinsic vibrissal curvature, roll and elevation affected the volume and surface area swept out by the whiskers.

Fig. 5 shows the results of this analysis. Two features of the figure are important to highlight. First, with the array at rest, the intrinsic curvature of the vibrissae significantly increases the volume enclosed by the array, from ~25 to ~36 cm^3, a 44% increase. Straight whiskers were simulated as described in Materials and methods. The increase in volume is largely a result of vibrissal curvature in the rostro-caudal direction. The rostral vibrissae are curved strongly concave forward, and the caudal vibrissae curve slightly concave backwards. These opposing directions of curvature cause the array to 'flare out' when viewed from above, increasing overall array volume.

Second, the effects of adding elevation and roll have mostly counterbalancing effects: during protraction, volume tends to increase when elevation is added but decrease when roll is added. Thus, the net effect on the volumetric search space of the rat of adding both roll and elevation to a whisk (as occurs during real behavior) is small (about 4%). The results for surface area were very similar to those for volume (data not shown).

Roll differentially changes the path lengths of dorsal and ventral vibrissae

Although roll and elevation do not have a significant effect on the overall size of the vibrissal search space, they have a large effect on the paths that individual whiskers take during protraction. We examined both the paths formed by the tips of the vibrissae, called 'tip traces', and the curved planes swept out by the entire arc length of a vibrissa during protraction.

When roll is added to simulations of whisking behavior, the lengths of the paths swept out by the vibrissa tips change across the vibrissal rows. Fig. 6A illustrates the difference between tip traces with and without roll for column two whiskers. It is clear that vibrissa tips in the dorsal rows trace out shorter paths with the addition of roll, while vibrissa tips in the ventral rows trace out longer paths.

Fig. 6B quantifies the differences in tip trace length across all vibrissae in the array. To make this figure, we calculated the tip trace length for each whisker in four whisking conditions: no roll and no elevation, roll only, elevation only, and both roll and elevation. For each whisker, we normalized these four lengths to the length generated by including both roll and elevation (this case therefore yielded a normalized length equal to unity). Then we computed the mean and s.d. for each of the four cases within each row. These means and s.d. are plotted in Fig. 6B. For the A-row of vibrissae (dorsal), the inclusion of roll decreases the tip trace lengths, while for the E-row of vibrissae (ventral), the roll increases the tip trace length.

Elevation alters the overall whisking angle, and ensures that the vibrissae explore non-overlapping spaces

Simulations showed that the addition of elevation to whisking has two separate effects. First, elevation causes the vibrissa tips to move more in line with the pitch of the rat's head. This effect is illustrated in Fig. 7A. In this figure the rat's head is shown in its standard

The Journal of Experimental Biology (2014) doi:10.1242/jeb.105338

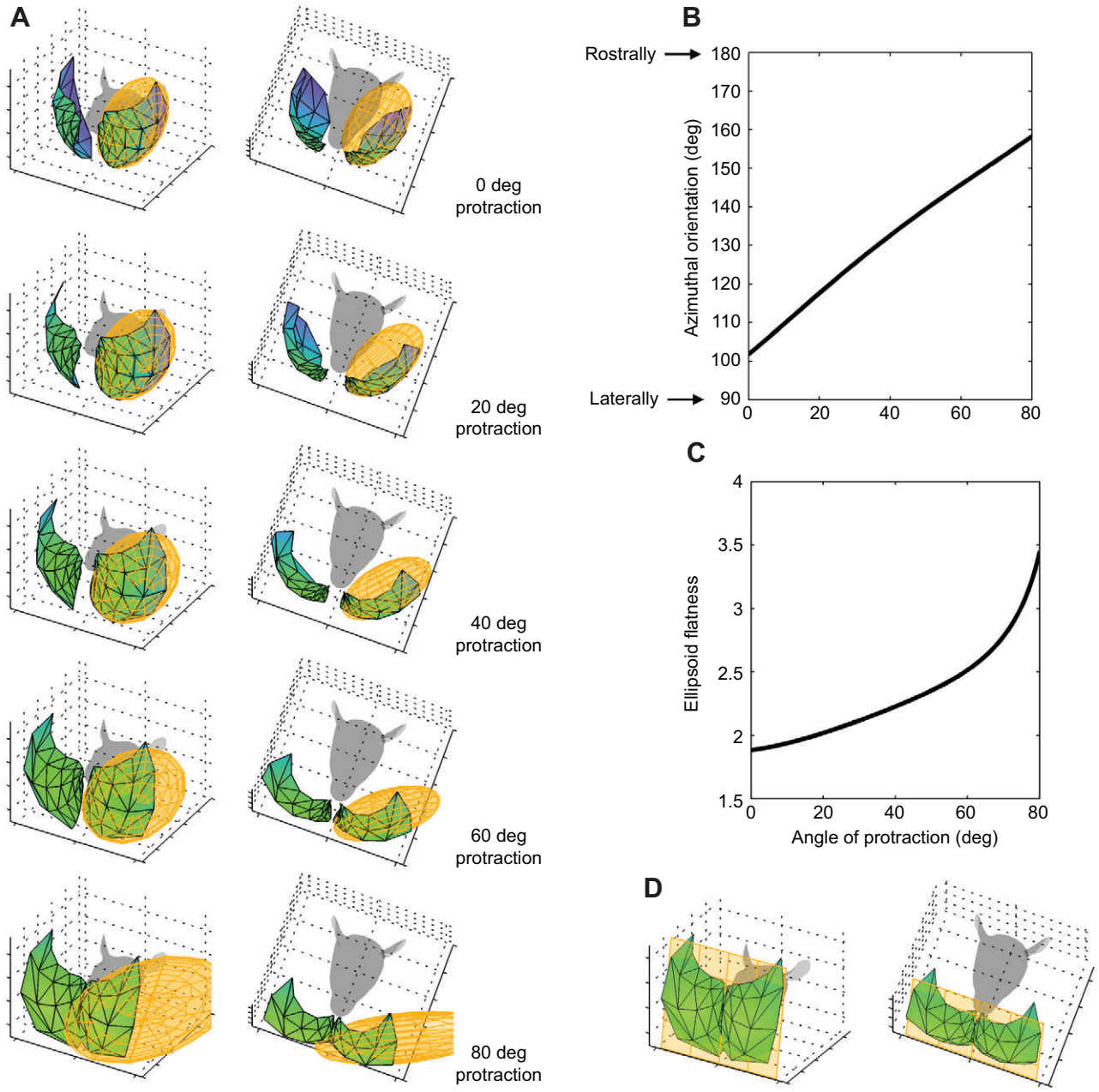

Fig. 4. As the rat protracts, the tips of the vibrissae form an ellipsoidal surface that changes its major axis from rostral–caudal to medio-lateral, and the surface formed by the tips flattens. (A) Change in the shape of the array during a protraction. The fit begins to break down near a protraction angle of θ=80 deg. (B) Change in azimuthal orientation of the ellipsoid during a protraction. Azimuthal orientation represents the angle of the vector normal to the largest face of the ellipsoid. The normal vector starts approximately perpendicular to the rat's face (~100 deg), and changes to point rostral–caudal (near 160 deg) at peak protraction. (C) The flatness of the ellipsoid, defined as the mean of the two longest radii divided by the shortest radius, increases during protraction. (D) Even at an extreme protraction angle of θ=80 deg, the tips of the vibrissae do not form a plane; an ellipsoidal fit is still significantly better.

orientation, with the rows of the whisker base points in the horizontal plane (Towal et al., 2011). In this orientation, the rat's head tilts upwards ~17 deg, as estimated from planes fitted by visual inspection to the top and bottom of the rat's head.

If elevation is omitted in simulations of whisking, the vibrissa tips tend not to move much out of the horizontal plane. The red traces of Fig. 7A show that the tip traces of the 'Greek' column and first column vibrissae form nearly horizontal lines when the whisk is simulated without elevation. The definition of the Greek column is standard, as described in Materials and methods. The purple traces of Fig. 7A show that the tilt of the tip traces increases considerably when elevation is added to the simulation. Across all whiskers, adding elevation to the simulations increased the median tip trace tilt from 3 to 17 deg, closely matching the angle of the head pitch.

Second, elevation decreases the redundancy of the space searched within the array. When elevation is omitted, the more caudal vibrissae within each row tend to explore the same space as the vibrissae immediately rostral to them. When elevation is added and the vibrissae protract, they tend to cover different spaces from the other vibrissae.

To quantify this effect, we developed a 'minimum distance' metric, which indicates how close a vibrissa is to the spaces

The Journal of Experimental Biology (2014) doi:10.1242/jeb.105338

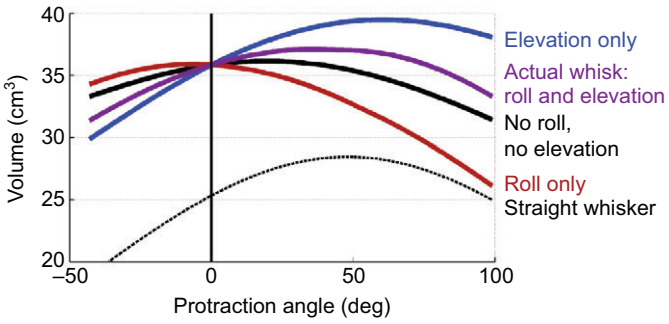

Fig. 5. The volume enclosed by the vibrissal array is minimally affected by changes in roll and elevation. A protraction angle of zero represents the vibrissal array at rest. Negative values represent retraction from the resting angle. The effects of elevation were included in the case of the straight whisker; roll has no effect on straight whiskers.

searched by all the other vibrissa. At each time step, the metric was defined as the minimum distance between the curve that defined the shape and position of one vibrissa and the 2D surfaces swept out by all the other vibrissae in the array. Intuitively, the minimum distance provides a measure of the amount of space any given whisker searches that is redundant with the past and present space searched by other whiskers. A small minimum distance indicates that the whisker is searching regions very close to regions that other whiskers have already explored, therefore limiting the total space explored by the array; a larger minimum distance means that the regions searched by individual whiskers are more distinct.

Fig. 7B illustrates the median of the minimum distances for all vibrissae on one side of the face throughout a protraction. The two cases that include elevation have significantly higher minimum distances than the two cases that do not.

The minimum distance as described here is obviously only one of a large number of metrics that could have been used to quantify the differences between the regions searched by the whiskers of the array. For example, we could have averaged the distance between one whisker and all the rest. We explored a variety of different metrics and found that they all yielded results similar to Fig. 7B provided that the history of the whisker trajectories was included. If whisker positions at only a single time step were used, there was little effect of adding roll and elevation.

Both volume and surface area are strongly correlated with spread but only weakly correlated with protraction angle and whisker spacing

The results above allowed us to estimate the shape of the surface formed by the vibrissa tips during whisking behavior as well as the volume enclosed by the array. When experimentalists record whisking behavior, however, they are often limited by a single camera view and are only able to track the position of the rostral-most and caudal-most whiskers on the two sides of the face. At every point during a whisk, the angular difference between the rostral- and caudal-most whiskers is termed the ‘spread’.

We therefore next used simulations to examine how this experimentally observable parameter, spread, was related to the search space of the rat. The area of the surface formed by the tips and the volume enclosed by the array were quantified as the vibrissae were moved through every physiologically possible configuration of average protraction angle (θ) and spread (see Materials and methods).

Fig. 8A shows that both volume and surface area are approximately linear with the spread of the array, regardless of protraction angle. The relationships are not completely linear, however, as can be seen by the width and color variations of the curves. For instance, a spread of 100 deg could mean that the volume is anywhere between 51 and 59 cm^3 depending on how far forward the array has protracted. Notably, the changes in volume due to changes in spread of the array (Fig. 8A) are much larger than changes due to roll and elevation (Fig. 5).

We next verified that the linear relationships between search space and spread were valid within the error bounds of the anatomical and kinematic models used in the simulations, representing the variability that might occur between rats. Both Towal et al. and Knutsen et al. (Towal et al., 2011; Knutsen et al., 2008) include error bounds on the locations of the base points of the vibrissae and the angles at which the vibrissae emerge from the mystacial pad. We deliberately chose parameter sets at the extremes of these error bounds in order to alter the search space of the vibrissal array.

We examined four extreme parameter sets. In the first set, the whisker angles were changed. The whisker angles include both the resting whisker angles and the slopes in Eqn 2A–E. These angles were all set to the outer edge of their error bounds such that the surface area and volume were maximized. In the second set, the whisker angles were changed in the same way as in the first set and, in addition, the base point positions were all shifted to the edge of their error bounds, again to maximize surface area and volume. The third and fourth sets were identical to the first two except that the parameters were shifted to the edge of the error bounds so as to minimize surface area and volume.

Fig. 8B plots the results of this analysis for the first two parameter sets, i.e. the ones that maximized surface area and volume. In this figure, volumes and surface areas have been normalized between zero and one to aid visual comparison. The figure reveals that all configurations of vibrissal morphology result in a linear relationship between spread and volume as well as a linear relationship between

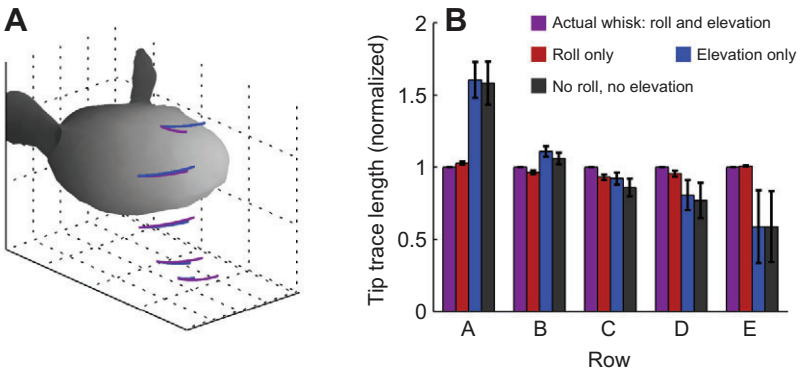

Fig. 6. The addition of roll decreases the length of tip traces during whisking for more dorsal rows and increases tip trace length in more ventral rows. (A) Tip traces for column 2 vibrissae for a 40 deg whisk. Purple traces represent whisking that includes both roll and elevation, and blue traces represent whisking that includes only elevation (no roll). (B) Tip trace lengths for all whiskers, averaged across columns. Error bars indicate the s.d. for each row. For each whisker, the trip trace lengths were normalized to the case that involves both roll and elevation, and values were then averaged within a row. For the A-row of vibrissae (dorsal), the tip traces without roll are much longer than the tip traces that include roll, while for the E-row of vibrissae (ventral), the tip traces that include roll are longer.

The Journal of Experimental Biology (2014) doi:10.1242/jeb.105338

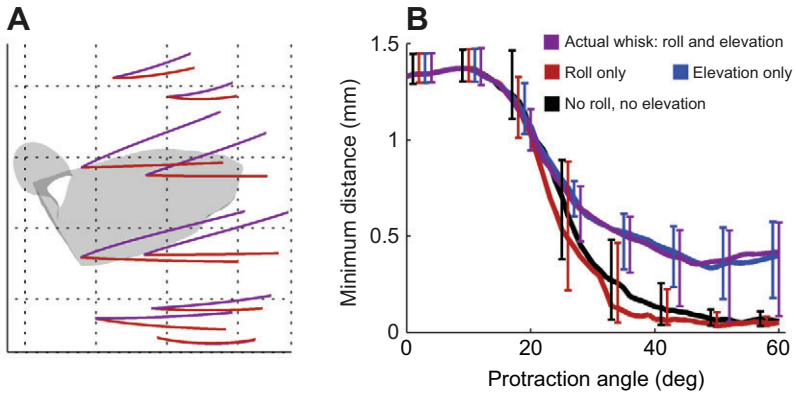

Fig. 7. Elevation causes the trajectories of the vibrissae tips to align more closely with the pitch of the head and reduces redundancy in the search space during a protraction. (A) The red traces show the trajectories of the tips of the Greek and first column vibrissae when the whisk is simulated without elevation (roll only). The purple traces show the same trajectories after elevation is added to the simulation. (B) Median distance indices for all vibrissae throughout a protraction. Error bars represent the upper and lower distance quartiles.

spread and surface area. In other words, the linearity of the relationship between spread and either volume or surface area is robust to errors in the vibrissal array model and thus to many of the variations that may occur across rats.

Although the linearity is robust, the magnitudes may change significantly. For instance, the nominal vibrissal configuration volume ranges from 11.9 to 78.3 cm^3, while the largest vibrissal configuration ranges from 21.7 to 109.0 cm^3, and the smallest ranges from 8.1 to 53.4 cm^3. The two extreme parameter sets that minimized (instead of maximized) surface area and volume yielded results very similar to those shown in Fig. 8B and therefore are not presented here.

We also assessed the effect of vibrissal spacing on surface area and volume. As described in Materials and methods, the spacing of the vibrissae within the array was allowed to vary according to linear, logarithmic or exponential distributions. The magnitudes for volume and surface area varied significantly between the different spacings – for large values of spread, they differed by as much as 15% – but the relationships between spread and volume and spread and surface area remained linear for all configurations. The linear relationship broke down only for exponential spacing combined with extremely large values of spread. Visual examination of this configuration confirmed that it does not look like a distribution of whiskers that would ever occur during natural whisking behavior.

To summarize, the analyses of this section have demonstrated three key features of the search space (volume and surface area) of the rat. First, the relationship between the size of the rat's search space and spread is generally linear and largely independent of protraction angle. Second, the linearity is robust to the individual variations likely to occur across rats. And third, the linearity is robust to the spacing of the vibrissae within the array.

Using spread as a proxy for volume and/or surface area

Although the strong linearity shown in Fig. 8 suggests that the spread of the array might be a reasonable proxy for estimating the search space of the rat, there are some important caveats.

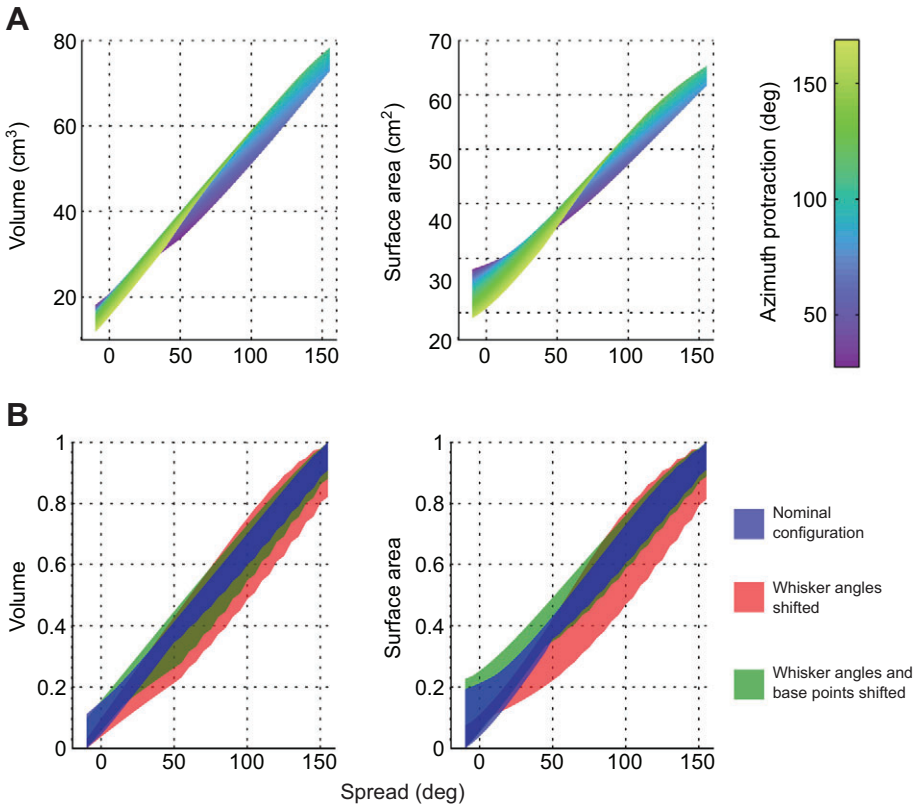

Fig. 8. The search space of the rat varies linearly with the spread of the array, and depends only weakly on protraction angle. (A) Both volume and surface area are weakly correlated with protraction angle but exhibit a strong linear correlation with spread. A spread of 0 deg indicates equal rostral and caudal angles. Note that a negative value of spread does not mean that the rostral whiskers are caudal to the caudal whiskers; it means the whiskers are bunched together. The color scale indicates the protraction angle, which ranges between 30 and 170 deg. (B) Normalized volume and surface area maintain a linear relationship with spread, even if the anatomical model is pushed to the extreme of its error bounds. In the two subplots, normalized volume and surface area are plotted as a function of spread for three different configurations of the model. The blue region shows results for the nominal configuration. The red region shows results when vibrissal orientation and kinematics are shifted to the edge of their error bounds to maximize surface area and volume. The green region shows results when vibrissal orientation, kinematics and basepoints were shifted to the edge of their error bounds, again to maximize surface area and volume.

Most importantly, the exact slope and intercept of the linear relationship will depend on the individual rat. The volume and surface area of a rat's whisker array will depend on the exact location of the base points, the length of the whiskers and the angles at which the whiskers emerge from the mystacial pad. Therefore, we do not recommend that experimentalists attempt to calculate the absolute magnitude of the volume or surface area directly from graphs such as those in Fig. 8A.

As an alternative to absolute magnitude, an experimentalist might like to obtain an estimate of relative changes in search space associated with a particular exploratory behavior. For example, if one observes a particular percent change in spread, one might ask what percent volume change has occurred. We can gain some insight into this question by noting that the slopes and intercepts of the graphs in Fig. 8 will always be positive, regardless of individual variations across rats. If we define the percent spread change as:

$$\%\text{Spread change} = 100 \times \frac{\left(\text{Final spread}\right) - \left(\text{Initial spread}\right)}{\left(\text{Initial spread}\right)}, \quad (1A)$$

then the percent change in the search space (volume or surface area) can be written as:

$$\%\text{Search space change} = \frac{\%\text{Spread change}}{1 + \frac{b}{m\left(\text{Initial spread}\right)}}, \quad (1B)$$

where m and b are the slope and intercept, respectively. Given that m and b will always be positive, Eqn 1A,B shows that the percent search space change (either percent volume or percent surface area) will always be smaller than the percent spread change.

The percent change in spread is thus an upper bound on the percent change in the search space of the rat. The rat will always experience smaller fractional change in sensing resolution than would be directly estimated from spread. Note that this effect occurs specifically because the intercept is non-zero – when the spread of the array is zero (rostral and caudal whiskers are at equal angles), the volume and surface area are both non-zero. If the intercept were zero, then the percent volume (or surface area) change during a whisk would be identical to the percent spread change.

The way in which spread can most accurately be used as a proxy for search space is to consider ratios of changes. For example, suppose that during a particular exploratory sequence, the spread changes by 35 deg during the first whisk, but by only 10 deg during the second whisk. In this case, we can say that the ratio of spread change between whisk one and whisk two is 35 deg/10 deg=3.5. We can then say with confidence that the ratio of the change in sensing resolution (as measured either by volume or surface area) is also equal to 3.5. As a second example, imagine that a particular change in spread during a whisk characterizes a particular exploratory behavior. We can then compare the change in sensing resolution during that behavior with the change in sensing resolution observed during other types of behavior.

Visualization of the rat's search space during natural whisking behaviors

We inserted behavioral data into the 3D anatomical model to visualize the rat's search space during natural exploratory behavior. Behavioral data were obtained from Towal and Hartmann (Towal and Hartmann, 2006), in which rats whisked freely in an empty environment to search for a reward. Movements of the rat's head and vibrissae were monitored and the positions of the rostral-most and caudal-most vibrissae were tracked along with the angular position of the head. For each video frame of behavioral data, the angles of the fourth and Greek vibrissa columns were mapped onto their respective columns in the 3D model. The remaining vibrissa columns were then linearly spaced within these two measured columns.

Fig. 9 shows a screenshot from supplementary material Movie 1 illustrating changes in spread, surface area and volume during a head rotation. The video underscores the multiple sources of variability in whisking, including variable right–left amplitudes, asymmetric spread changes and rostral–caudal amplitude and phase differences.

DISCUSSION

Shape of the array around the face at rest and during a protraction

When at rest, the tips of the mystacial vibrissae extend completely around the head, both above and below it. The vibrissae thus cover both the eyes and mouth, immediately suggesting that the vibrissa tips define an envelope for sensing physical intrusions into the space surrounding these important structures. Although likely to be true, this protective interpretation cannot represent the entire story, as it overlooks other important geometric features of the whisker array.

To explain these geometric features, we must make a clear distinction between the centroid of the vibrissal tips and the center of the fit to the vibrissal tips. This distinction is schematized in two dimensions in Fig. 10A. The centroid of the tips is the average position of the tips. In contrast, the center of the tips is the point from which all the tips are approximately equidistant. As shown in Fig. 10B, with the vibrissae at rest, the centroid is located at the rat's mouth, while the center is located at the midpoint between the rat's eyes (cf. Fig. 2).

The centering of the vibrissal tips about the eyes may represent a peripheral correlate of the neural registration of the tactile and visual systems found in structures such as the superior colliculus (McHaffie and Stein, 1982; Dauvergne et al., 2004; Bezdudnaya and Castro-Alamancos, 2011). This geometric arrangement will inherently tend to ensure that tactile and visual modalities operate within the same coordinate system and bring tactile and visual maps into registration. This registration could facilitate a 'hand-off' between visual and tactile systems as the rat approaches an object.

The particular arrangement of whiskers revealed in the present study would also allow them to play a key role in predatory behavior. The distribution of vibrissal tips weighted about the mouth suggests their importance in prey capture (Anjum et al., 2006; Munz et al., 2010). When the vibrissae are at rest, the centroid of their tips falls nearly exactly at the mouth, but during whisking the centroid moves just rostral to the mouth (Fig. 3B), exactly where the rat would target potential prey.

In accordance with the rostral motion of the centroid during protraction, the ellipsoidal fits to the tips also tended to orient more rostrally and become flatter (Figs 3, 4). Given that whisker locations are likely to indicate the rat's current focus of attention (Mitchinson and Prescott, 2013), these fits suggest that the rat's attention is directed rostrally at the time of peak protraction.

Although the geometric fits to the array are most compactly expressed in polar coordinates, there is no reason to assume that the rat itself employs a polar coordinate system during exploration. In fact, the vibrissal tips come close to forming a plane at peak protraction (Fig. 4D), and the rat could potentially operate in

The Journal of Experimental Biology (2014) doi:10.1242/jeb.105338

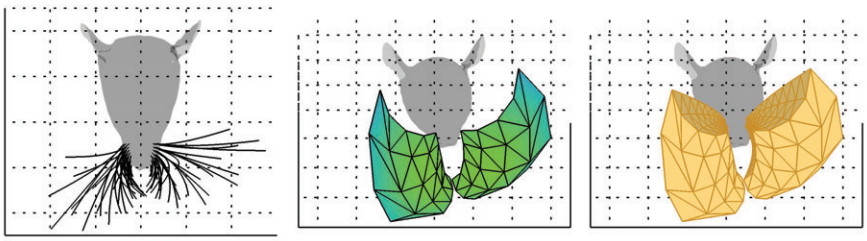

Fig. 9. Screenshot from supplementary material Movie 1, illustrating spread, surface area and volume during head turning asymmetry. The left panel shows a top-down view of whisking behavior with all movements of the head subtracted. The center panel shows the surface area formed by the tips, and the right panel illustrates the volume encompassed by the two sides of the array.

Cartesian coordinates, as humans may do during reaching behavior (Morasso, 1981; Soechting and Lacquaniti, 1981).

Volume and surface area as measures of the rat's search space

The search space of the rat can be described either as the volume encompassed by the whisker array or as the surface area formed by the tips of the vibrissae. The size of the search space provides insight into the spatial resolution desired for particular sensing behaviors: a larger search space indicates that the rat is sacrificing high resolution spatial data, while a smaller search space suggests a requirement for increased spatial resolution.

It is therefore important to have an estimate of changes in the size of the search space across behaviors. Previous studies have used spread as an estimate of these changes because this metric is easy to quantify experimentally. The present work demonstrates a close linear relationship between spread and volume as well as between spread and surface area. The linearity of these relationships is surprisingly independent of protraction angle, but the exact values depend on the slopes and intercepts shown in Fig. 8, which can vary considerably across individual rats.

These results have three consequences. First, the magnitude of the spread cannot, in general, be used to directly estimate the magnitude of the volume or surface area. Second, the percent change observed in spread will always represent an upper bound on the percent change in either volume or surface area. Third, the ratios of changes in spread will always be the same as the ratios of changes in search space. As shown in the example of head turning asymmetry, if a particular change in spread Δ_1 is associated with behavior 1, and a particular change in spread Δ_2 is associated with behavior 2, then the ratio of the volume and surface area changes between the behaviors will be the same as the ratio of the spread changes, Δ_1/Δ_2.

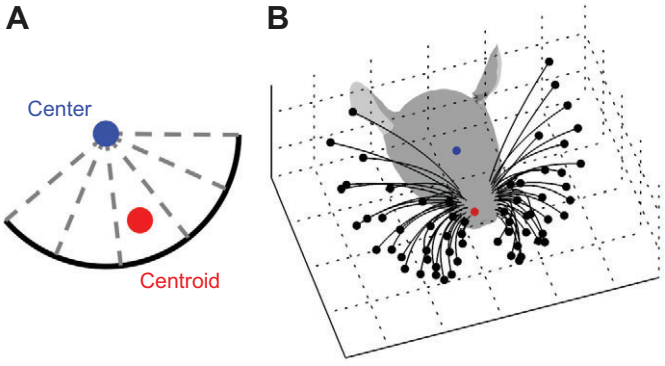

Fig. 10. The distinction between the centroid of the vibrissal tips and the center of the fit to the vibrissal tips. (A) A 2D example of the distinction between the centroid and the center. The centroid of the black curve, illustrated by a red dot, is the average of all the points on the black curve. The center of a circular fit to the black curve is shown as a blue dot. The center is the point from which all the points on the black curve are equidistant (gray dashed lines). (B) Now extending to three dimensions, the centroid of the vibrissal tips lies near the rat's mouth, while the center of the fit to the vibrissal tips lies near the eyes.

Whisking kinematics: effects of intrinsic curvature, roll and elevation

Rat vibrissae have a distinct intrinsic curvature that approximates a parabola (Knutsen et al., 2008; Towal et al., 2011; Quist and Hartmann, 2012). The intrinsic curvature was found to increase the volume of the rat's search space by over 40% compared with straight whiskers. In contrast, the addition of roll and elevation to the kinematics of whisking has only a modest effect on the size of the search space.

Roll and elevation were, however, found to significantly affect the trajectories of the whisker tips. With the addition of roll, vibrissal tips in the ventral rows trace out longer trajectories, and vibrissal tips in the dorsal rows trace out shorter trajectories (Fig. 6). The addition of elevation changes in whisking has two effects. First, it ensures that vibrissal tips follow a path spatially aligned with the rat's head. Second, it decreases the redundancy of the space searched within the array. Without elevation, a vibrissa often explores the same space as the whisker directly rostral to it has already explored. Thus, the elevation component of whisking may serve as a means to increase the rat's efficiency during search without significantly increasing the energy expended (MacIver et al., 2010).

Kinematic variability in whisking

The present study examined the search space of the rat only during non-contact whisking behavior. More complex kinematics may occur when the rat whisks against an object. Despite this added complexity, the tightly linear relationship between search space and spread (Fig. 8) will hold regardless of whether the animal is touching an object or not. As stated above, we anticipate that the rat will reduce its search space when its goal is to explore an object with high spatial resolution.

Because search space is so tightly correlated with spread, the rat's sensing resolution is in turn primarily determined by its differential control over rostral and caudal vibrissae. An important open question is thus the degree to which rostral–caudal kinematic variability reflects voluntary control. Previous biomechanical models of the intrinsic muscles have predicted that more anterior whiskers will protract less than the others in the row (Simony et al., 2010), but the patterns of muscle activation that might underlie the rat's voluntary ability to differentially modulate rostral and caudal amplitude are poorly understood. Future models of rodent facial musculature would permit investigation of the mechanisms for the rat's voluntary control of whisking patterns and identify the biomechanical constraints that limit the variability of these patterns.

MATERIALS AND METHODS

Model of the rat head and vibrissal array at rest

The 3D morphology of the rat head and vibrissal array at rest was based on Towal et al. (Towal et al., 2011) and Knutsen et al. (Knutsen et al., 2008).

The Journal of Experimental Biology (2014) doi:10.1242/jeb.105338

The morphology included the positions of the vibrissal base points and the shapes and orientations of the vibrissae.

Fig. 11A illustrates the head placed in standard position and orientation. Fig. 11B–D illustrates the three angles that describe the orientation of the vibrissa as it emerges from the mystacial pad at rest. As in previous studies (Knutsen et al., 2008; Towal et al., 2011), these angles are defined according to the proximal, linear portion of the whisker as it emerges from the mystacial pad.

The azimuthal angle (θ) represents the vibrissa's angle of emergence in the horizontal plane, Elevation (φ) describes the vibrissa's angle of emergence relative to the horizontal plane. The torsional rotation or roll of a vibrissa about its own axis is described by ζ.

As will be described below, the Knutsen et al. (Knutsen et al., 2008) dataset provides slightly different values for the resting elevation angles than does Towal et al. (Towal et al., 2011). Therefore, all analyses concerning the vibrissal array at rest were performed twice, once using resting elevation values from Towal et al. and once using resting elevation values from Knutsen et al.

Modeling a whisk: equations

The simulations in the present study required us to combine judiciously morphological and kinematic datasets from two different laboratories. The study of Towal et al. (Towal et al., 2011) provides values for all angles of emergence of all the vibrissae: θ_{rest}, φ_{rest} and ζ_{rest}. All values were obtained from the euthanized animal. The study of Knutsen et al. (Knutsen et al., 2008) provides values only for φ_{rest}, not for θ_{rest} or ζ_{rest}. The Knutsen et al. study also identifies the slopes of the relationships between θ and φ and between θ and ζ during whisking motion in the awake, behaving animal. These slopes are presented in table 1 of Knutsen et al. (Knutsen et al., 2008). Based on these slopes, we can write equations that describe how the vibrissae will roll and elevate as a function of protraction angle, θ. These relationships are represented in Eqn 2A–E. These equations were used in all simulations of whisking behavior throughout the present study.

Row A:

$$\zeta = -0.76 \times (\theta - \theta_{rest}) + \zeta_{rest}$$
$$\varphi = 0.12 \times (\theta - \theta_{rest}) + \varphi_{rest} . \quad (2A)$$

Row B:

$$\zeta = -0.25 \times (\theta - \theta_{rest}) + \zeta_{rest}$$
$$\varphi = 0.30 \times (\theta - \theta_{rest}) + \varphi_{rest} . \quad (2B)$$

Row C:

$$\zeta = 0.22 \times (\theta - \theta_{rest}) + \zeta_{rest}$$
$$\varphi = 0.30 \times (\theta - \theta_{rest}) + \varphi_{rest} . \quad (2C)$$

Row D:

$$\zeta = 0.42 \times (\theta - \theta_{rest}) + \zeta_{rest}$$
$$\varphi = 0.14 \times (\theta - \theta_{rest}) + \varphi_{rest} . \quad (2D)$$

Row E:

$$\zeta = 0.73 \times (\theta - \theta_{rest}) + \zeta_{rest}$$
$$\varphi = -0.02 \times (\theta - \theta_{rest}) + \varphi_{rest} . \quad (2E)$$

Modeling a whisk: the animation tool PuppetMaster

The basis for all simulations was the morphological model RatMap, publically available for download as supplementary information to Towal et al. (Towal et al., 2011). Implementing Eqn 2A–E directly through RatMap, however, would be a laborious process because it would require us to input every whisker orientation angle at every time step for every whisker.

We therefore developed a whisking animation tool called PuppetMaster that outputs the position of the whiskers given a desired protraction angle. The main outputs of PuppetMaster are the *x*-, *y*- and *z*-coordinates for all nodes of all desired whiskers for all time steps. PuppetMaster also allows the user to alter the spacing and shape of the whiskers as well choose whether the simulation should include changes in roll and elevation over the course of the whisk. PuppetMaster is available on request from the corresponding author.

Calculating surface area and volume of the array

Fig. 12A illustrates the morphology of the rat head and vibrissal array. As shown in Fig. 12B, the surface area of the array was calculated as the area formed by connecting the tips of the vibrissae on each side of the rat's face.

We defined the volume of the array to encompass all vibrissae from the Greek to the fourth column on each side of the rat's face. As is standard in the field, the Greek vibrissae are identified as the four most caudal whiskers in the array. These whiskers are slightly offset in the dorsal–ventral direction relative to the five rows, identified by letters A–E. We used the method of pyramids (Zordan et al., 2006) to find the volume of the vibrissal array, as schematized in Fig. 12C,D. Eqn 3 expresses the total volume of the solid as a sum of the volumes of the individual pyramids.

$$\sum_{i}^{N} \frac{1}{3} h_i \left(\frac{1}{2} \left| \mathbf{u}_i \times \mathbf{v}_i \right| \right) . \quad (3)$$

In Eqn 3, N is the number of pyramids, $\mathbf{u}_i$, and $\mathbf{v}_i$ are vectors describing two of the sides of the base of the ith pyramid, and h_i is the height of the ith pyramid.

In one analysis (Fig. 5), we aimed to examine the effect of intrinsic vibrissal curvature on the search space of the rat. Straight vibrissae were

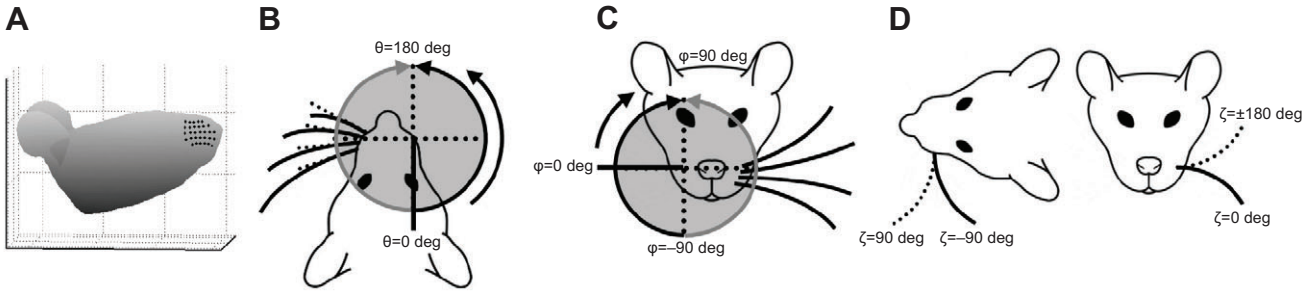

Fig. 11. Coordinate systems for the rat head and vibrissal array. (A) Standard position and orientation of the head. The rat's nose is placed at the origin (0, 0, 0), and the head is pitched so that on average the rows of vibrissal base points lie parallel to the *x*–*y* plane. The mid-sagittal plane is the *y*–*z* plane, and the positive *y*-direction points from caudal to rostral. The pitch of the head is defined so that the average plane of the whisker rows is parallel to the *y*-axis. In this orientation, the rat's head is pitched upwards by about 17 deg. (b) Three angles, θ, φ and ζ, describe the orientation of each vibrissa at rest as it emerges from the mystacial pad. The horizontal (azimuthal) angle θ represents the angle of emergence in the horizontal plane, with θ=0 deg pointing caudal and θ=180 deg pointing rostral. The primary whisking motion occurs in θ. The elevation angle φ is the angle of emergence relative to the horizontal plane. A vibrissa that emerges horizontally from the rat's cheek is at φ=0 deg, and a vibrissa emerging straight upwards is at φ=90 deg. The roll angle ζ gives the angle of rotation about the vibrissa's own axis, with 0 deg concave downwards, 90 deg concave forwards, 180 deg concave upwards and −90 deg concave backwards (adapted from Towal et al., 2011).

The Journal of Experimental Biology

modeled to emerge from the mystacial pad at the same angle as the curved vibrissae and extend out in a straight line. The length of each straight vibrissa was the same as the arc-length of its curved counterpart.

Spread and spacing of the vibrissae

In the context of the vibrissal system, spread is defined as the azimuthal angle difference between the rostral-most and caudal-most vibrissae (Grant et al., 2009). In the simulations of the present study, spread was defined as the angle of the Greek column subtracted from the angle of the fourth column. With the whiskers at rest, spread is ~40 deg.

In one analysis (Fig. 8), we aimed to determine how the protraction angle θ and the spread of the array independently affected surface area and volume. We therefore positioned the model of the vibrissal array in a wide range of configurations defined by two parameters: the average protraction angle of the array and the spread of the array. We varied θ between 30 and 170 deg, and varied the spread between −10 and 155 deg. The Greek column vibrissae were constrained to lie between 5 and 175 deg, and the fourth column vibrissae between 25 and 190 deg. Because we independently varied θ and spread, we are confident that we have captured the relationships between volume, surface area, spread and protraction angle for every possible (θ, spread) configuration of the whiskers.

The 'spacing' of the vibrissae is defined by the difference in angles between adjacent columns in the array. In one analysis (described in Results, Both volume and surface area are strongly correlated with spread, but only weakly correlated with protraction angle and whisker spacing), we tested the effects of spacing on surface area and volume. To run these tests, we compared three different spacing distributions. In 'linear spacing', the angular difference between each adjacent column was set equal. In 'logarithmic spacing', the angular difference between adjacent columns followed a logarithmic distribution, and in 'exponential spacing', the angular difference followed an exponential distribution.

Spherical, ellipsoid and planar fits, error analysis and perceptually balanced colormaps

Spherical and ellipsoidal fits to the vibrissae tips were performed using the MATLAB function 'ellipsoid_fit' (Petrov, 2009), which exploits a least squares minimization. Planar fits were performed using principal component analysis and the geometric mean of the data points.

Errors were defined as the smallest Euclidean distances from the vibrissa tips to the surface of the sphere, ellipsoid or plane. To determine significance in error difference across multiple fits, the errors were passed through the Box–Cox transformation to give them a normal distribution and then compared using Student's *t*-test.

Several figures in the present work make use of the perceptually scaled CubicYF colormap based on cubic-law luminance. This colormap is derived in the PMKMP function (Niccoli, 2010).

Acknowledgements

We thank R. Blythe Towal for contributions to the initial conceptualization of the study and for finding the reference to the 'method of pyramids' that allowed us to compute the volume of the array. We thank Chris S. Bresee for many helpful discussions on neuroethology.

Competing interests

The authors declare no competing financial interests.

Author contributions

M.J.Z.H. and L.A.H. conceived the study and designed the simulations, and L.A.H. performed them. M.J.Z.H. and L.A.H. analyzed the data and wrote the manuscript.

Funding

This work was supported by National Science Foundation (NSF) awards IOS-0818414, NSF CAREER IOS-0846088 and NSF EFRI-0938007 to M.J.Z.H.. L.A.H. received support from Department of Defense, Air Force Office of Scientific Research, National Defense Science and Engineering Graduate (NDSEG) Fellowship, 32 CFR 168a.

Supplementary material

Supplementary material available online at
http://jeb.biologists.org/lookup/suppl/doi:10.1242/jeb.105338/-/DC1

References

Anjum, F., Turni, H., Mulder, P. G. H., van der Burg, J. and Brecht, M. (2006). Tactile guidance of prey capture in Etruscan shrews. *Proc. Natl. Acad. Sci. USA* **103**, 16544-16549.

Berg, R. W. and Kleinfeld, D. (2003). Rhythmic whisking by rat: retraction as well as protraction of the vibrissae is under active muscular control. *J. Neurophysiol.* **89**, 104-117.

Bermejo, R., Vyas, A. and Zeigler, H. P. (2002). Topography of rodent whisking – I. Two-dimensional monitoring of whisker movements. *Somatosens. Mot. Res.* **19**, 341-346.

Bezdudnaya, T. and Castro-Alamancos, M. A. (2011). Superior colliculus cells sensitive to active touch and texture during whisking. *J. Neurophysiol.* **106**, 332-346.

Carvell, G. E. and Simons, D. J. (1990). Biometric analyses of vibrissal tactile discrimination in the rat. *J. Neurosci.* **10**, 2638-2648.

Carvell, G. E. and Simons, D. J. (1995). Task- and subject-related differences in sensorimotor behavior during active touch. *Somatosens. Mot. Res.* **12**, 1-9.

Dauvergne, C., Ndiaye, A., Buisseret-Delmas, C., Buisseret, P., Vanderwerf, F. and Pinganaud, G. (2004). Projections from the superior colliculus to the trigeminal system and facial nucleus in the rat. *J. Comp. Neurol.* **478**, 233-247.

Deutsch, D., Pietr, M., Knutsen, P. M., Ahissar, E. and Schneidman, E. (2012). Fast feedback in active sensing: touch-induced changes to whisker-object interaction. *PLoS ONE* **7**, e44272.

Fee, M. S., Mitra, P. P. and Kleinfeld, D. (1997). Central versus peripheral determinants of patterned spike activity in rat vibrissa cortex during whisking. *J. Neurophysiol.* **78**, 1144-1149.

Gao, P., Bermejo, R. and Zeigler, H. P. (2001). Whisker deafferentation and rodent whisking patterns: behavioral evidence for a central pattern generator. *J. Neurosci.* **21**, 5374-5380.

Grant, R. A., Mitchinson, B., Fox, C. W. and Prescott, T. J. (2009). Active touch sensing in the rat: anticipatory and regulatory control of whisker movements during surface exploration. *J. Neurophysiol.* **101**, 862-874.

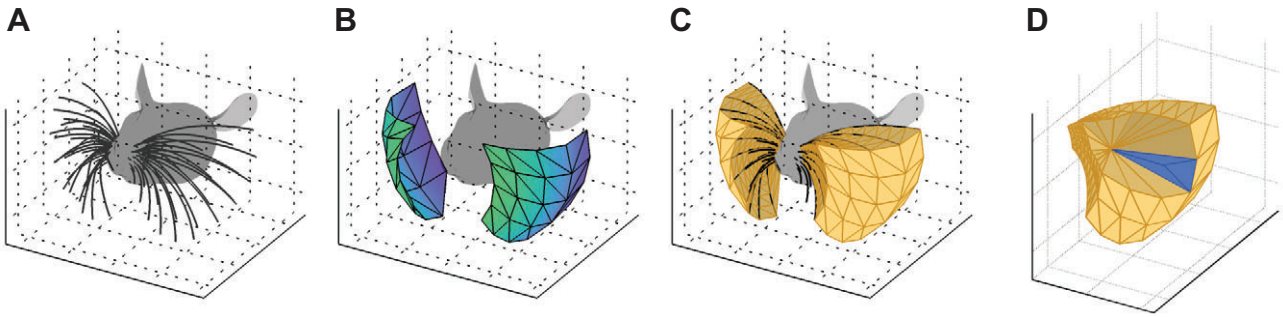

Fig. 12. Calculating the surface area and volume of the vibrissal array. (A) The morphology of the array from Towal et al. (Towal et al., 2011). (B) Surface area of the array formed by the vibrissal tips of the Greek to the fourth columns. Color represents rostral–caudal distance from the origin. (C) Volume formed by the Greek to the fourth columns of the array. (D) A cutaway schematic diagram illustrates that the volume of the array can be calculated by the method of pyramids (Zordan et al., 2006). One pyramid is highlighted in blue. The method has three steps. First, the surface of the solid is split into triangles, forming a triangular mesh. Second, a point in the middle of the solid is defined as the apex of all the triangular pyramids whose bases form the solid's surface. Third, because all the pyramids share the same apex and the triangular sides are all adjacent, the volume of the solid can be found by summing the volumes of all the pyramids.

Grant, R. A., Sperber, A. L. and Prescott, T. J. (2012). The role of orienting in vibrissal touch sensing. *Frontiers in Behavioral Neuroscience* **6**, 39.
Harvey, M. A., Bermejo, R. and Zeigler, H. P. (2001). Discriminative whisking in the head-fixed rat: optoelectronic monitoring during tactile detection and discrimination tasks. *Somatosens. Mot. Res.* **18**, 211-222.
Knutsen, P. M., Biess, A. and Ahissar, E. (2008). Vibrissal kinematics in 3D: tight coupling of azimuth, elevation, and torsion across different whisking modes. *Neuron* **59**, 35-42.
MacIver, M. A., Patankar, N. A. and Shirgaonkar, A. A. (2010). Energy-information trade-offs between movement and sensing. *PLOS Comput. Biol.* **6**, e1000769.
McHaffie, J. G. and Stein, B. E. (1982). Eye movements evoked by electrical stimulation in the superior colliculus of rats and hamsters. *Brain Res.* **247**, 243-253.
Mitchinson, B. and Prescott, T. J. (2013). Whisker movements reveal spatial attention: a unified computational model of active sensing control in the rat. *PLOS Comput. Biol.* **9**, e1003236.
Mitchinson, B., Martin, C. J., Grant, R. A. and Prescott, T. J. (2007). Feedback control in active sensing: rat exploratory whisking is modulated by environmental contact. *Proc. Biol. Sci.* **274**, 1035-1041.
Morasso, P. (1981). Spatial control of arm movements. *Exp. Brain Res.* **42**, 223-227.
Munz, M., Brecht, M. and Wolfe, J. (2010). Active touch during shrew prey capture. *Frontiers in Behavioral Neuroscience* **4**, 191.
Niccoli, M. (2010). Perceptually improved colormaps. *MATLAB Central File Exchange* 28982.
Petrov, Y. (2009). Ellipsoid fit. *MATLAB Central File Exchange* 24693.
Quist, B. W. and Hartmann, M. J. Z. (2012). Mechanical signals at the base of a rat vibrissa: the effect of intrinsic vibrissa curvature and implications for tactile exploration. *J. Neurophysiol.* **107**, 2298-2312.
Sachdev, R. N. S., Berg, R. W., Champney, G., Kleinfeld, D. and Ebner, F. F. (2003). Unilateral vibrissa contact: changes in amplitude but not timing of rhythmic whisking. *Somatosens. Mot. Res.* **20**, 163-169.
Sellien, H., Eshenroder, D. S. and Ebner, F. F. (2005). Comparison of bilateral whisker movement in freely exploring and head-fixed adult rats. *Somatosens. Mot. Res.* **22**, 97-114.
Simony, E., Bagdasarian, K., Herfst, L., Brecht, M., Ahissar, E. and Golomb, D. (2010). Temporal and spatial characteristics of vibrissa responses to motor commands. *J. Neurosci.* **30**, 8935-8952.
Soechting, J. F. and Lacquaniti, F. (1981). Invariant characteristics of a pointing movement in man. *J. Neurosci.* **1**, 710-720.
Towal, R. B. and Hartmann, M. J. (2006). Right-left asymmetries in the whisking behavior of rats anticipate head movements. *J. Neurosci.* **26**, 8838-8846.
Towal, R. B. and Hartmann, M. J. Z. (2008). Variability in velocity profiles during free-air whisking behavior of unrestrained rats. *J. Neurophysiol.* **100**, 740-752.
Towal, R. B., Quist, B. W., Gopal, V., Solomon, J. H. and Hartmann, M. J. Z. (2011). The morphology of the rat vibrissal array: a model for quantifying spatiotemporal patterns of whisker-object contact. *PLOS Comput. Biol.* **7**, e1001120.
Vincent, S. B. (1913). The tactile hair of the white rat. *J. Comp. Neurol.* **23**, 1-34.
Welker, W. I. (1964). Analysis of sniffing of the albino rat. *Behav. Brain Res.* **22**, 223-244.
Wineski, L. E. (1983). Movements of the cranial vibrissae in the Golden hamster (*Mesocricetus auratus*). *J. Zool.* **200**, 261-280.
Wineski, L. E. (1985). Facial morphology and vibrissal movement in the golden hamster. *J. Morphol.* **183**, 199-217.
Zordan, V. B., Celly, B., Chiu, B. and DiLorenzo, P. C. (2006). Breathe easy: model and control of human respiration for computer animation. *Graph. Models* **68**, 113-132.